Solar Energy
And Sustainable Development
Refereed, biannual scientific journal issued by:
The Libyan Center for Solar Energy Research and Studies

Optimizing CZTS Solar Cell Performance with Advanced Layer Configurations Using SCAPS Simulation

Oussama Belhaidouri[1]*, Rachida Moultif[2], Laila Mouakkir[3], Sanaa Rochd[4], Ahmed Hader[5], Khadija Mhada[6].

[1,2,4]Laboratory Of Condensed Matter Physics,Faculty Of Sciences Ben m'sik ,Casablanca ,Morocco.
[3]Physics departement ,Polymer physics , Mechanical sciences and materials laboratory , Faculty of sciences ben m'sik ,Casablanca ,Morocco.
[5]Regional Center for Education and Training Professions,Casablanca-Settat,Settat Establishment, Morocco.
[6]ISPS2I Laboratory, ENSAM, Hassan II University , Casablanca , Morocco.

E-*mail:* [1] oussbelhaidouri@gmail.com ,[2] rachidamoultif09@gmail.com ,[3] mouakkir_laila@yahoo.fr ,
[4] rochd.sanaa91@gmail.com ,[5] ahader73@yahoo.fr ,[6] Khadijamhada1@gmail.com .

SPECIAL ISSUE ON:

The 2024 1st International Conference on Materials Sciences and Mechatronics for Sustainable Energy and the Environment
October 1-3, 2024 at Béni-Mellal, Morocco

KEYWORDS

CZTS solar cells; SCAPS simulation; transition metal dichalcogenides; MoS_2; ZnO; thermal effects; renewable energy.

ABSTRACT

This research analyzes the modeling of CZTS (Copper Zinc Tin Sulfide) solar cells, with a focus on advanced layer configuration and thermal management to improve operational efficiency. Using SCAPS-1D software, this investigation seeks to augment cell efficiency by fine-tuning the dimensions of absorptive layers, modifying buffer compositions, and adjusting other critical components. The study evaluates the role of transition metal dichalcogenides (TMDs), specifically MoS_2 as the hole transport layer and ZnO as the window layer, in influencing open-circuit voltage (Voc) and short-circuit current density (Jsc).

Furthermore, the research delves into temperature-related effects, demonstrating that elevated temperatures lead to a decrease in Voc and Jsc attributable to bandgap narrowing and heightened recombination processes. Through the optimization of the thicknesses of the CZTS, MoS_2, and WSe_2 layers, this study elucidates the manner in which material adjustments influence Voc, Jsc, fill factor (FF), and overall efficiency (η). In addition, effective thermal management emerges as a critical factor, given that increased temperatures elevate recombination rates, thereby adversely affecting FF and efficiency. The results of this study provide essential information for increasing the performance, durability and stability of CZTS solar cells under various environmental conditions.

*Corresponding author.

DOI: https://doi.org/10.51646/jsesd.v14iSI_MSMS2E.399

تحسين كفاءة الخلايا الشمسية (كبريتيد النحاس والزنك والقصدير) من خلال تطوير التكوينات الطبقية المتقدمة وتحليل الأداء باستخدام برنامج سكابسالاسماء باللغة العربية.

ملخص: تحلل هذه الدراسة نمذجة الخلايا الشمسية (كبريتيد النحاس والزنك والقصدير)، مع التركيز على تكوينات طبقية متقدمة وإدارة حرارية لتحسين الكفاءة التشغيلية. باستخدام برنامج (سكابس-1د)، تهدف هذه الدراسة إلى تعزيز كفاءة الخلايا من خلال تعديل أبعاد الطبقات الماصة، وتعديل تركيبات الطبقات العازلة، وضبط مكونات أخرى حاسمة. تقيم الدراسة دور ثنائي كبريتيد المعادن الانتقالية، خاصة ثنائي كبريتيد الموليبدينوم كطبقة نقل للثقوب وأكسيد الزنك كطبقة نافذة، في التأثير على جهد الدائرة المفتوحة وكثافة تيار الدائرة القصيرة. علاوة على ذلك، تتناول الدراسة تأثيرات درجات الحرارة، مما يظهر أن ارتفاعها يؤدي إلى انخفاض جهد الدائرة المفتوحة وكثافة تيار الدائرة القصيرة بسبب تضييق فجوة الطاقة وزيادة عمليات إعادة التركيب. من خلال تحسين سماكة طبقات كبريتيد النحاس والزنك والقصدير وثنائي كبريتيد الموليبدينوم وسيلينيد التنجستن، توضح الدراسة كيف تؤثر تعديلات المواد على جهد الدائرة المفتوحة وكثافة تيار الدائرة القصيرة وعامل التعبئة والكفاءة الإجمالية. بالإضافة إلى ذلك، تبرز الإدارة الحرارية الفعالة كعامل حاسم، حيث يؤدي ارتفاع درجات الحرارة إلى زيادة معدلات إعادة التركيب، مما يؤثر سلبًا على عامل التعبئة والكفاءة. تقدم نتائج هذه الدراسة معلومات أساسية لزيادة الأداء والموثوقية والاستقرار للخلايا الشمسية كبريتيد النحاس والزنك والقصدير تحت ظروف بيئية مختلفة.

الكلمات المفتاحية – الخلايا الشمسية كبريتيد النحاس والزنك والقصدير؛ محاكاة سكابس؛ ثنائي كبريتيد المعادن الانتقالية؛ ثنائي كبريتيد الموليبدينوم؛ أكسيد الزنك؛ التأثيرات الحرارية؛ الطاقة المتجددة.

1. INTRODUCTION

Photovoltaic solar cells convert solar energy into electricity by exploiting the principles of the photovoltaic effect in p-n junctions [1-3]. Thin-film photovoltaic cells, known for their high optical absorption coefficients, require only a few micrometers of material to enable significant light absorption [4-6]. This reduced thickness provides flexibility to the devices, making them suitable for applications on curved surfaces, such as in automobiles or wearable technologies. In addition, reducing the thickness of the absorber layer allows for ultra-thin and semi-transparent cells, offering promising prospects for their integration into building-integrated photovoltaic systems.

Although CIGS (copper indium gallium selenide) and CdTe (cadmium telluride) solar cells currently dominate the thin-film technology sector, they face major challenges. CIGS relies on rare and expensive materials such as indium (In) and gallium (Ga), while CdTe contains toxic elements such as cadmium (Cd) and tellurium (Te), raising concerns about their environmental impact and long-term sustainability. This highlights the urgent need to develop alternative, abundant, non-toxic, and economically viable materials without compromising performance. In this context, CZTS (copper zinc tin sulfide) is positioned as a promising candidate for future generations of thin-film photovoltaic cells [7-10].

CZTS has many advantages as a photovoltaic material: it is composed of elements abundant in the Earth's crust, it is non-toxic and inexpensive (copper, zinc, tin, and sulfur), making it an attractive material for large-scale sustainable photovoltaic applications. Unlike rare and toxic materials, CZTS offers a reduced environmental footprint and has high potential for adoption in renewable energy technologies. Moreover, its direct bandgap of about 1.5 eV is ideal for solar energy conversion, as it falls within the optimal range of bandgaps for efficient light absorption in the solar spectrum [11]. Its absorption coefficient, over 10^4 cm^{-1}, enables efficient light capture even with thin films, which is crucial for reducing material usage and manufacturing costs [12].

Solar cells based on CZTS also exhibit remarkable stability under changing environmental conditions, such as temperature fluctuations, a key criterion for ensuring reliable long-term operation in real-world applications [13]. Furthermore, its tunable optoelectronic properties, such as its adjustable bandgap and high hole mobility, make it a versatile material that can be

optimized to meet various performance requirements. These characteristics, combined with the fact that CZTS does not rely on any rare or toxic elements, make it a prime candidate for environmentally responsible and scalable photovoltaic technologies [14,15].

In this study, CZTS was selected due to its potential to overcome the limitations of existing thin-film technologies while providing a sustainable and efficient alternative for renewable energy. The main objective of this research is to optimize the performance of CZTS-based solar cells using advanced layer configurations and appropriate thermal management, in order to address the low open-circuit voltage (Voc) that currently limits their efficiency. By fine-tuning the material layers and integrating innovative buffer layers as well as hole transport layers, this work aims to maximize the performance of CZTS-based cells, positioning them as viable alternatives for future photovoltaic systems.In order to rectify this diminished Voc and augment the efficacy of CZTS-based solar cells, this research emphasizes the utilization of copper-based (p-type) inorganic semiconductors as prospective hole transport layers (HTLs). These substances exhibit high hole mobility, excellent electrical conductivity, high optical transparency, cost-effectiveness and environmental sustainability, making them promising candidates for increasing the performance of solar cells [15].

In our modeling methodology, we utilized SCAPS-1D (Solar Cell Capacitance Simulator in 1 Dimension) software to simulate the performance of CZTS-based photovoltaic cells, designed with a sophisticated i-ZnO/WSe_2/CZTS architecture. SCAPS-1D was chosen for this study due to its robust capabilities in modeling the electro-optical properties of thin-film solar cells. It enables precise analysis of critical performance metrics, such as current-voltage characteristics, band alignment, and recombination processes within multilayer photovoltaic structures. This makes it an ideal tool for evaluating potential efficiency and optimizing the design of each layer within the solar cell. Each material in this cell architecture was meticulously selected for its distinct properties and functional significance. CZTS (Copper Zinc Tin Sulfide) serves as the light-absorbing layer due to its ideal direct bandgap of approximately 1.5 eV, which closely aligns with the optimal value for solar energy conversion. Its high absorption coefficient enhances the cell's ability to capture sunlight and generate electron-hole pairs efficiently, making it a strong candidate for effective light absorption and energy conversion. Furthermore, CZTS is composed of earth-abundant, non-toxic elements, positioning it as an environmentally sustainable and economically feasible alternative to conventional absorber materials such as CIGS (Copper Indium Gallium Selenide) or CdTe [15].

The i-ZnO (intrinsic zinc oxide) layer functions as the window layer, characterized by a substantial bandgap of roughly 3.3 eV. La large bande interdite offre une transparence élevée, permettant une pénétration maximale de la lumière avec une perte d'absorption minimale, augmentant ainsi encore le courant de court-circuit.

The monolayer tungsten diselenide (WSe_2) was selected as the buffer layer owing to its outstanding properties, which render it highly advantageous for cutting-edge applications in nanoelectronics, spintronics, and valleytronics. WSe_2 is particularly distinguished among all recognized monolayer transition-metal dichalcogenides (TMDs) by its exceptional spin splitting and prolonged valley coherence time. These features, in conjunction with its superior band alignment with CZTS, facilitate efficient charge separation and mitigate recombination losses. Furthermore, WSe_2 operates as a direct bandgap semiconductor with an energy gap of 1.2 eV, thereby augmenting its applicability for photovoltaic purposes. Our incorporation of high-quality monolayer WSe_2 within the simulation framework capitalizes on its advanced electronic characteristics, as substantiated by high-resolution angle-resolved photoemission spectroscopy (ARPES), to increase the overall efficiency of the device.

MoS_2 (molybdenum disulfide) acts as the hole transport layer (HTL), recognized for its elevated carrier mobility and suitable band alignment, thereby promoting effective hole extraction and

transport. This, in turn, which results in increased open-circuit voltage (Voc) and fill factor. Through the integration of these materials into our SCAPS model, we systematically evaluated their influence on device efficiency, providing invaluable insights for optimizing layer configurations and informing experimental designs aimed at further increasing solar cell performance.

2. METHODOLOGY

2.1. Simulation

Numerical analysis has emerged as an essential approach in advancing and refining a range of technological devices, with a specific focus on thin-film solar cells (TFSCs).By employing sophisticated simulation frameworks such as SCAPS 1D, investigators are able to meticulously forecast and optimize the operational performance and energy efficacy of these solar cells in relation to a wide range of environmental factors. This methodology not only promotes a more profound comprehension of the complex physical phenomena occurring within the cells but also permits the discernment of optimal material compositions and architectural designs, thereby contributing to increased device reliability, efficiency, and adaptability to practical applications. SCAPS 1D 3.307, which was developed in the year 2012 by the Department of Electronics and Information Systems (ELIS) at the University of Gent, was specifically engineered to emulate the characteristics of the field layer and blaze diffractive grating in Thin-Film Solar Cells (TFSCs). The software is constructed upon a robust foundation of scholarly research and empirical evidence, incorporating an extensive array of meticulously cited parameters. A significant parameter within SCAPS is the pre-factor A_α, established at 10^5 to calibrate the absorption coefficient obtained from a designated equation. This value is substantiated by scholarly investigations, including those conducted by Burgelman (1999) and Liang et al. (2018). [16-18].

$$\alpha = A_\alpha (hv - E_g)^{\frac{1}{2}} \qquad (1)$$

The simulation is executed under solar irradiance conditions equivalent to 1 Sun, defined by a power density of 1000 W/m² and a thermal environment maintained at 300 K. This approach incorporates the application of well-established theoretical constructs, including the continuity equation, Poisson's equation, and the equations governing electron and hole transport, which collectively elucidate various recombination mechanisms. The primary aim of these analytical endeavors is to accurately capture and reproduce the operational characteristics exhibited by thin-film solar cells (TFSCs) . The execution of these simulations is crucial for optimizing both the design parameters and operational performance of TFSCs, with the ultimate goal of achieving optimal efficiency alongside economic feasibility. As the global appetite for renewable energy solutions intensifies, the use of numerical analysis software, such as SCAPS 1D, is expected to gain increased significance in the ongoing evolution of sustainable energy technologies.[19].

$$\frac{\partial n}{\partial t} = \frac{1}{q} div\vec{J}_n + G_n - R_n \qquad (2)$$

$$\frac{\partial p}{\partial t} = \frac{1}{q} div\vec{J}_p + G_p - R_p \qquad (3)$$

When simulating thin-film solar devices, it is essential to consider the global discontinuity parameter. However, a recent study did not include this essential parameter, instead choosing to use electrical and optical values from existing literature while keeping the temperature fixed at 300 K. The solar cell was illuminated with a global spectrum of 1000 W/m² and an air mass value of 1.5, based on previous research. Additionally, the input material properties for each layer and the device parameters in the 1-D SCAPS tool were adjusted as needed. Despite the omission of the

global discontinuity parameter, this approach provided valuable insights into the performance of thin-film solar devices. Future research should incorporate the global discontinuity parameter to increase the accuracy of the simulation results.

2.2. Device configuration

This computational tool is predicated upon mathematical formulations that are relevant to semiconductor physics, specifically focusing on the continuity equation governing electron dynamics (4), the continuity equation applicable to hole transport (5), and the Poisson equation [20]:

$$\frac{\partial j_n}{\partial x} + G_n - U_n(n,p) = 0 \qquad (4)$$

$$\frac{\partial j_p}{\partial x} + G_p - U_p(n,p) = 0 \qquad (5)$$

$$\frac{d^2\psi}{d^2x} = \frac{dE}{dx} = -\frac{\rho}{\varepsilon_r \varepsilon_0}(p - n + N_D^+ - N_A^-) \qquad (6)$$

The following equations describe how electrons and holes drift and scatter during carrier transport:

$$j_n = qn\mu_n E + qD_n \frac{\partial n}{\partial x} \qquad (7)$$

$$j_p = qn\mu_p E + qD_p \frac{\partial p}{\partial x} \qquad (8)$$

The relationship between scattering efficiency, career mobility, and career lifetime is defined by Einstein's equation:

$$D_{(n,p)} = \sqrt{\mu_{(n,p)} \frac{KT}{q} \tau_{(n,p)}} \qquad (9)$$

The efficiency (PCE) and the fill factor are showing as:

$$FF = \frac{P_{max}}{P_t} = \frac{V_{max} J_{max}}{V_{oc} I_{sc}} \qquad (10)$$

$$PCE = \frac{V_{oc} I_{sc}}{P_{in}} FF \qquad (11)$$

The illustrated model delineates a complex stratified architecture of a CZTS (Copper Zinc Tin Sulfide) photovoltaic cell, meticulously engineered for simulation utilizing the SCAPS (Solar Cell Capacitance Simulator) software. This configuration incorporates a sequence of deliberately organized layers, each fulfilling a pivotal function in increasing the efficiency and performance of the solar cell. Positioned at both the uppermost and lowermost regions of the architecture are Au (Gold) contacts, which are imperative for facilitating the conduction of electrical current throughout the cell. These contacts guarantee effective charge collection and transport, which are indispensable for the holistic energy conversion mechanism. Situated beneath the upper contact is the i-ZnO (Intrinsic Zinc Oxide) layer, which serves as a buffer layer.

This layer is essential for increasing the interface between the WSe_2 layer and the frontal contact, thus augmenting electron transport and reducing recombination losses. The WSe_2 layer is subsequently positioned as the window layer. Its fundamental purpose is to facilitate maximal light transmission while contributing to the photovoltaic effect through the promotion of electron-hole pair generation.

Figure 1. the structure of the proposed device.

The principal component of the structure is CZTS absorber layer, which serves as the absorber layer tasked with the capture of solar radiation and its conversion into electrical energy. CZTS is particularly beneficial due to its abundance and non-toxic nature, rendering it a promising candidate for sustainable energy applications. Beneath the CZTS layer lies the MoS_2 (Molybdenum Disulfide) layer, which functions as a back contact or hole transport layer. This layer is pivotal in promoting the mobility of holes and increasing charge separation, thereby increasing the efficiency of the cell [21]. Finally, the TCO (Transparent Conductive Oxide) layer is located at the base of the structure, Figure 1. It offers both transparency for optimal light absorption and electrical conductivity, thereby ensuring effective charge transport throughout the device. This comprehensive simulation framework utilizing SCAPS enables researchers to rigorously investigate the performance attributes of CZTS solar cells, allowing them to meticulously adjust various parameters and emulate diverse environmental conditions. the device and material parameters utilized in this study, chosen based on experimental data, literature values, theoretical considerations, or reasonable estimates, are presented in Table 1 [22-24].

Table 1. The parameters used in this simulation.

Parameter	**CZTS**	**MoS_2**	**WSe_2**	**i-ZnO**
thickness (μm)	Var	1	Var	0.08
dielectric permittivity (relative)	10	3	13.8	8.9
Electron mobility ($cm^2/V.s$)	100	100	30	10
hole mobility ($cm^2/V.s$)	25	150	30	10
shallow uniform donor density ND (cm^{-3})	10	10	10^{17}	10^{20}
shallow uniform acceptor density NA (cm^{-3})	2×10^{16}	10^{17}	0	0
bandgap (eV)	1.50	1.29	1.55	3.65
Nc (cm^{-3})	2.2×10^{18}	2.2×10^{18}	8.3×10^{18}	5.2×10^{18}
Nv (cm^{-3})	1.8×10^{19}	1.8×10^{19}	1.4×10^{19}	1×10^{19}
electron affinity (eV)	4.5	4.2	4.03	4.8
Electron thermal velocity (cm/s)	10^7	10^7	1.7×10^7	2×10^7
hole thermal velocity (cm/s)	10^7	10^7	1.4×10^7	10^7

3. RESULTS

3.1. Analyzing the influence of the thickness of the absorber layer

In Figure 2, the SCAPS simulations illustrate the impact of varying the thickness of the CZTS layer on the photovoltaic properties of the solar cell. An observable trend emerges in both the open-circuit voltage (Voc) and the short-circuit current density (Jsc) as the layer thickness is incrementally increased.

At an initial thickness of 0.2857 µm, the solar cell achieves a Voc of 0.78177 V along with a significant Jsc of 31.68 mA/cm². indicating efficient light absorption and charge collection, this efficiency is attribued to the minimal recombination losses characteristic of the thinner layer. With an increase in thickness to 0.5714 µm, Voc increases to 0.7947 V, which signifies a reduction in surface recombination and an improvement in charge separation efficiency. Conversely, Jsc experiences a decrement to 31.21 mA/cm², likely resulting from the augmentation of resistive and recombination losses within the bulk of the thicker material.

As the thickness of 0.8571 µm, Voc peaks at 0.80981 V, which signifies further advancements in charge separation capabilities. Notably, Jsc continues to decrease to 29.06 mA/cm², indicating a trade-off between augmented absorption and heightened recombination losses. As the thickness escalates to 1.143 µm, Voc stabilizes at 0.82003 V, whereas Jsc diminishes further to 28.24 mA/cm², indicating that increased layer thickness may exacerbate resistive losses, thus adversely affecting current density.

For thicknesses above 1.429 µm, Voc continues to increase, reaching a maximum of 0.83964 V at 2 µm. This increase can be attributed to a reduction in recombination sites, which increases the voltage output. Nonetheless, Jsc demonstrates a downward trajectory, ultimately reaching 27.83 mA/cm² at 2 µm, suggesting that, while thicker layers may increase voltage through diminished recombination, they concurrently restrict current generation due to elevated internal resistance and absorption inefficiencies.

In summation, the findings highlight the importance of optimizing the CZTS layer thickness to balance between Voc and Jsc for the attainment of maximum operational efficiency. The modeling results emphasize the necessity of fine-tuning the thickness of the absorber layer to realize an optimal compromise between increased voltage and minimized current losses, which is crucial for the improvement of CZTS solar cell performance [25–28].

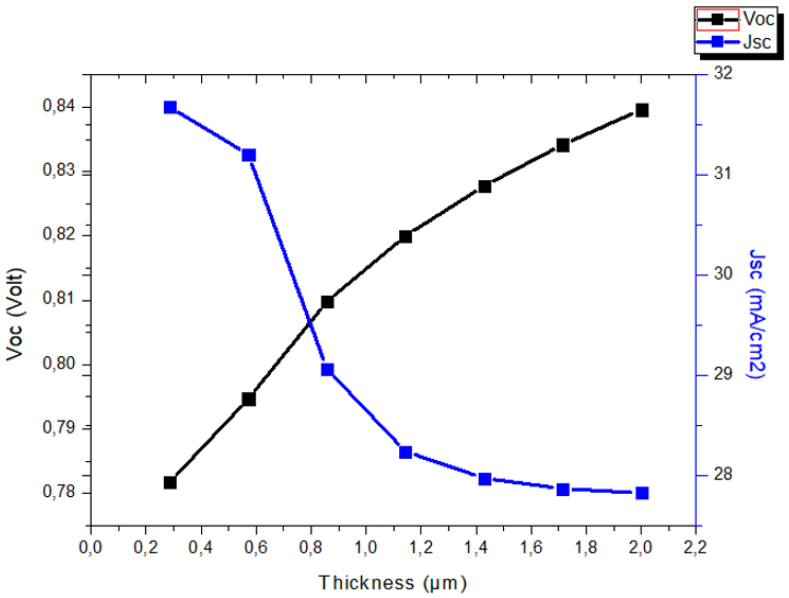

Figure 2. Variation of cell efficiency Jsc and Voc with CZTS thickness.

In Figure 3, the SCAPS simulation results for the CZTS solar cell reveal a nuanced relationship between the thickness of the absorber layer and pivotal performance indicators: fill factor (FF) and efficiency (η). As the thickness of the CZTS layer varies, these parameters manifest distinct tendencies that highlight the intricate relationship between material characteristics and device efficacy.

At initial thickness of 0.2857 µm, the cell achieves a fill factor of 70.61% and an efficiency of 17.49%. This observation implies proficient charge transport and minimal resistive losses, thereby facilitating effective energy conversion. Nevertheless, as the thickness escalates to 0.5714 µm, both FF and efficiency experience a decline to 68.80% and 17.06%, respectively. This decline points signifies heightened recombination and resistive losses, which may hinder charge collection.

Upon reaching a thickness of 0.8571 µm, there is a partial recovery in FF to 70.90%, while efficiency diminishes to 16.69%. This observation suggests that, while some resistive losses are mitigated, the increased thickness may still introduce additional recombination sites, negatively impacting overall device performance. At a thickness of 1.143 µm,, the FF further increases to 72.43%, with efficiency stabilizing at 16.77%, suggesting a compromise between increased charge collection and persistent recombination phenomena.

Beyond this juncture, at a thickness of 1.429 µm, the FF continues to ascend, attaining 73.06%, while efficiency realizes a modest rise to 16.92%. This improvement implies that the thickness of the absorber layer is approaching an optimal equilibrium wherein the advantages of increased light absorption begin to surpass the disadvantages associated with increased recombination. At the maximum thickness of 2 µm, the FF reaches its zenith at 73.56%, and efficiency rebounds to 17.19%, emphasizing the successful attenuation of recombination losses and the improvement of charge transport.

In summation, these findings accentuate the significance of fine-tuning the thickness of the CZTS layer to optimize both FF and η. Attaining the appropriate thickness is imperative for maximizing the efficiency of CZTS solar cells, as it reconciles light absorption, charge separation, and loss mechanisms within the device [29].

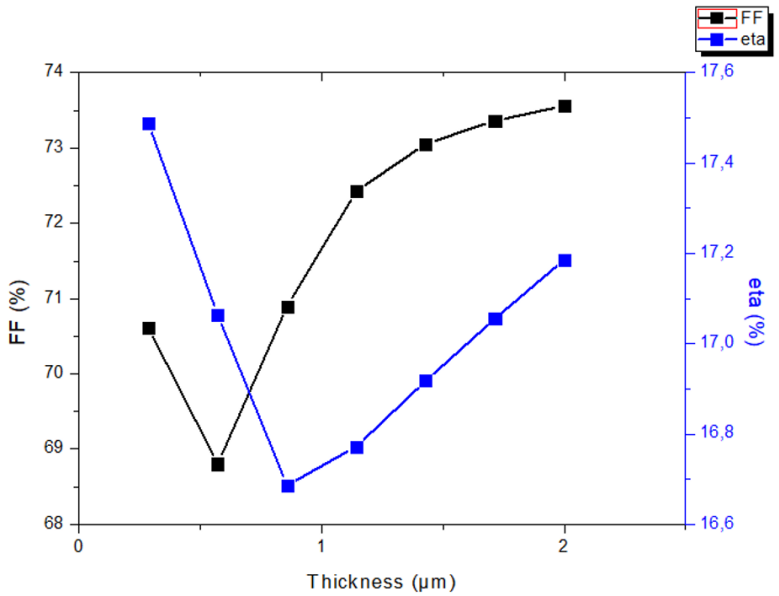

Figure 3. Variation of cell efficiency eta and FF with CZTS thickness.

3.2. Analyzing the influence of the thickness of interfacial layer

In Figure 4, the SCAPS model simulation demonstrates the effect of the MoS_2 layer thickness on the open-circuit voltage (Voc) and short-circuit current density (Jsc) of the photovoltaic device.

As the layer thickness is augmented, both Voc and Jsc demonstrate upward trajectories, indicative of improvements in charge separation and light absorption efficiency.

Initially, at a thickness of 0.1667 µm, Voc is measured at 0.79945 V, and Jsc is recorded at 26.39 mA/cm². demonstrating effective initial charge separation and collection mechanisms. When the thickness is increased to 0.3333 µm, Voc ascends to 0.80354 V, while Jsc reaches 26.81 mA/cm², implying a reduction in recombination losses and a concomitant improvement in absorption characteristics. At a thickness of 0.5 µm, Voc persists in its upward trend, attaining a value of 0.80709 V, with Jsc achieving 27.28 mA/cm². This observation denotes an optimal equilibrium between absorption efficacy and diminished recombination phenomena. Further augmentation of thickness to 0.8333 µm yields a Voc of 0.81291 V and a Jsc of 28.16 mA/cm², thereby reflecting ongoing advancements in charge separation dynamics. For thicknesses at 1 µm and greater, both Voc and Jsc continue to exhibit an upward trajectory, culminating in values of 0.82125 V and 29.38 mA/cm² at a thickness of 1.5 µm, respectively. This indicates that increased layer thickness facilitates superior light absorption, thereby increasing current generation while concurrently minimizing recombination losses. In summary, the optimization of the MoS_2 layer thickness is essential for the maximization of both Voc and Jsc. The observed upward trends signify that increased thickness not only increases charge separation but also augments light absorption, resulting in increased performance of the solar cell as delineated in the SCAPS model [30-31].

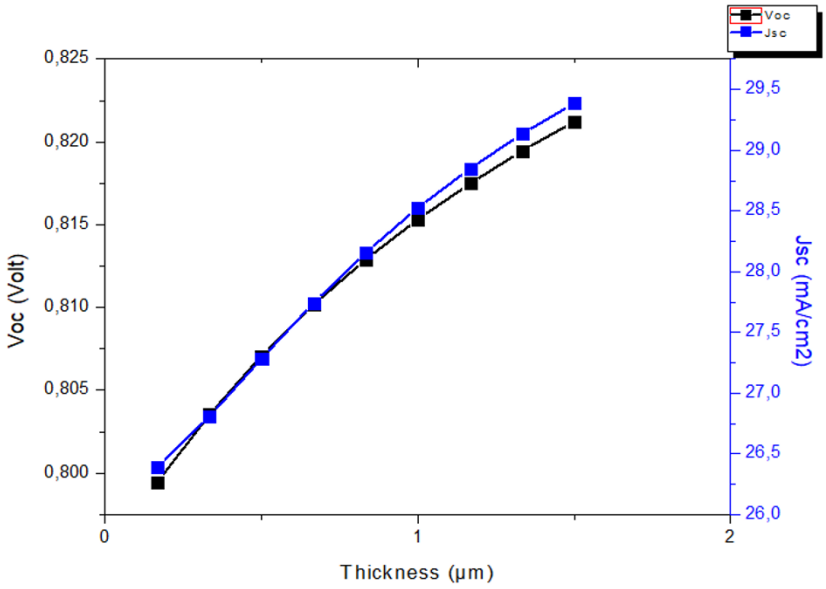

Figure 4. Variation of cell efficiency Jsc and Voc with interfacial layer.

In Figure 5, the SCAPS simulation results demonstrate how the thickness of the MoS_2 layer affects both the fill factor (FF) and the efficiency (η) of the solar cells. As the MoS_2 layer thickness increases, the FF tends to decrease, while the efficiency (η) shows an upward trend.

At an initial thickness of 0.1667 µm, the FF is relatively high at 73.53%, indicating efficient charge transport with minimal resistive losses. However, as the thickness increases, the FF gradually decreases, reaching 71.34% at 1.5 µm. This decline suggests that thicker MoS_2 layers may introduce additional resistive losses or recombination sites, thereby reducing the efficiency of charge carrier extraction.

In contrast, the efficiency starts at 15.51% and steadily rises to 17.22% as the thickness reaches 1.5 µm. This increase in efficiency is likely due to increased light absorption and increased charge generation in thicker layers. The additional material may allow for better photon capture, compensating for the negative effects observed on the FF. In conclusion, the results reveal a

trade-off between FF and efficiency (η) as the thickness of the MoS_2 layer increases. While thicker layers increase light absorption and thus efficiency, they also present challenges in charge transport, leading to a reduction in FF. Therefore, optimizing the thickness of the MoS_2 layer is crucial to balancing these effects and maximizing the overall performance of CZTS solar cells modeled with SCAPS [31].

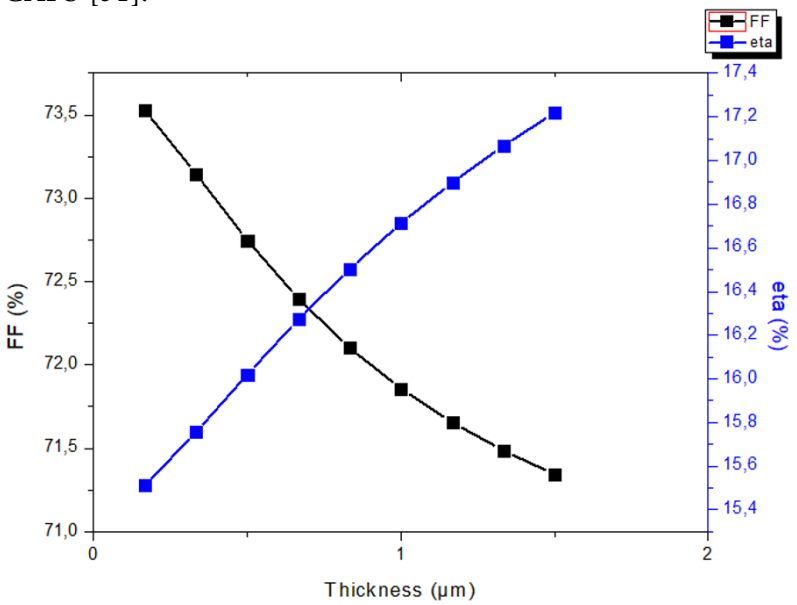

Figure 5. Variation of cell efficiency FF and eta with interfacial layer.

3.3. Analyzing the influence of the thickness of buffer layer

In Figure 6, the SCAPS simulation results illustrate a complex interrelationship between the thickness of the WSe_2 layer and critical performance metrics, including open-circuit voltage (Voc) and short-circuit current density (Jsc). As the thickness of the WSe_2 layer is augmented, Voc demonstrates a marginally positive trajectory, stabilizing at approximately 1 µm. This observation implies an improvement in charge separation and a reduction in recombination at optimal thickness values. In contrast, Jsc encounters a decrement with the increase in thickness, presumably attributable to elevated recombination losses or hindered carrier transport within thicker layers.

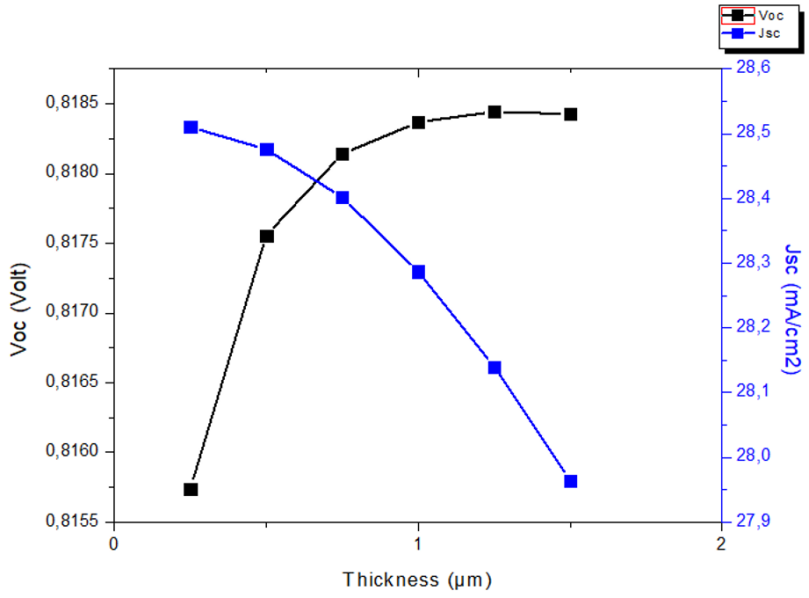

Figure 6. Variation of cell efficiency Voc and Jsc with buffer layer.

The compromise between these performance parameters suggests that an optimal WSe_2 thickness exists near 1 µm, wherein Voc reaches its zenith without imposing significant adverse effects on Jsc. Furthermore, the initial improvements in the fill factor (FF) and efficiency (η) concomitant with increasing thickness indicate increased device performance, which subsequently plateaus, thereby illustrating a equilibrium between effective charge collection and recombination. This examination emphasizes the criticality of meticulous optimization of layer thickness in the pursuit of high-efficiency solar cells [32].

The modeling of the solar cell structure using SCAPS provides in Figure 7 how the thickness of the WSe_2 layer impacts both the fill factor (FF) and the efficiency (η) of the device. As the thickness of the WSe_2 layer increases, both FF and η show a notable improvement initially. This indicates increased charge collection efficiency and a reduction in series resistance, which collectively contribute to increased overall device performance.

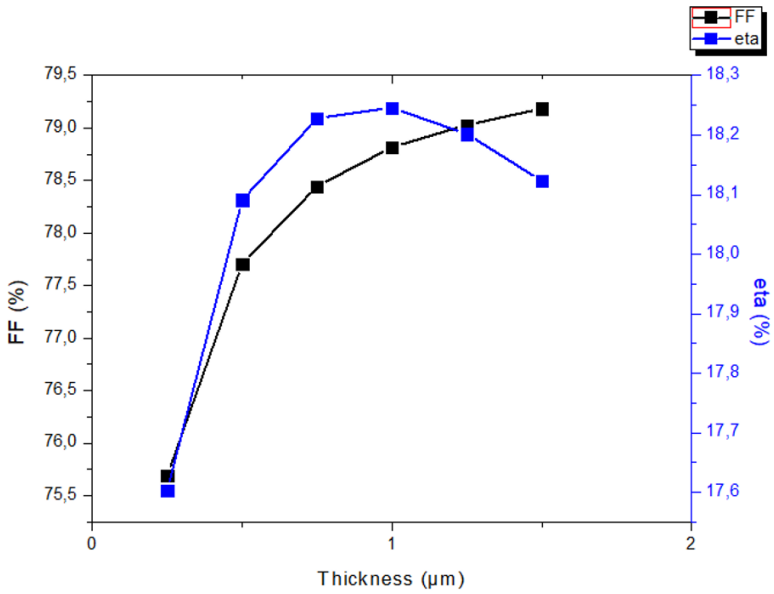

Figure 7. Variation of cell efficiency FF and eta with buffer layer.

The FF increases significantly as the thickness approaches 1 µm. This suggests that the electrical characteristics of the device, such as reduced internal resistance and increased carrier transport, are optimized at this thickness. The peak in FF around this point indicates that the device operates more efficiently, with better charge extraction and lower recombination rates at the electrodes.

The efficiency follows a similar trend, peaking alongside the FF. This peak efficiency reflects the balance between maximizing photovoltaic conversion and minimizing losses due to recombination and resistive pathways. The optimal thickness allows for sufficient light absorption while maintaining efficient charge carrier separation and transport, crucial for high photovoltaic performance.

As the thickness exceeds the optimal point, both FF and η experience slight declines. This can be attributed to increased recombination losses or resistive losses that outweigh the benefits of additional light absorption. Thicker layers may lead to longer carrier paths, increasing the likelihood of recombination before charge extraction.

This detailed analysis underscores the importance of precise thickness optimization in the WSe_2 layer to achieve high efficiency in solar cells. It highlights the delicate balance necessary between light absorption, charge transport, and recombination dynamics in designing efficient photovoltaic devices [32].

3.4. Analyzing the influence of temperature

In Figure 8 , the SCAPS simulation results represents the thermal dependence of the open-circuit voltage (Voc) and short-circuit current density (Jsc) for a solar cell composed of CZTS, arranged in the configuration of i-ZnO/WSe_2/CZTS/MoS_2. As the temperature increases from 300 K to 400 K, both Voc and Jsc exhibit downward trends, a common characteristic in photovoltaic systems. The open-circuit voltage (Voc) manifests a considerable decline from approximately 0.815 V at 300 K to 0.668 V at 400 K. This observed behavior is predominantly ascribed to the temperature-dependent characteristics of the bandgap energy. With an increase in temperature, the bandgap of the absorber material (CZTS, in this instance) diminishes, consequently leading to a reduction in Voc. Moreover, the augmented thermal energy facilitates an increase in the intrinsic carrier concentration, which subsequently elevates the saturation current (I_0). Given that Voc is logarithmically correlated to the ratio of the photocurrent to the saturation current, a rise in I_0 culminates in a diminished Voc. This temperature-induced reduction in Voc serves to reflect the intrinsic thermodynamic constraints of the semiconductor material employed in the solar cell. The short-circuit current density (Jsc) similarly experiences a decline with the increase in temperature, albeit the decrease is less pronounced in comparison to Voc, diminishing from approximately 28.525 mA/cm² at 300 K to 27.102 mA/cm² at 400 K. The observed reduction in Jsc can be attributed to multiple factors. Elevated temperatures expedite carrier recombination phenomena, particularly within the bulk of the absorber layer and at the interfaces, thereby leading to a decrease in the quantity of photogenerated carriers that contribute to the current. As temperature escalates, phonon scattering becomes increasingly prominent, which results in a diminished mobility of charge carriers (i.e., electrons and holes). This reduction in mobility can obstruct the effective collection of carriers at the electrodes, thereby yielding a lower Jsc. Additionally, elevated temperatures may exacerbate energy losses due to carrier thermalization, wherein the excess kinetic energy of photogenerated carriers is dissipated as heat prior to their contribution to the current[33-35].

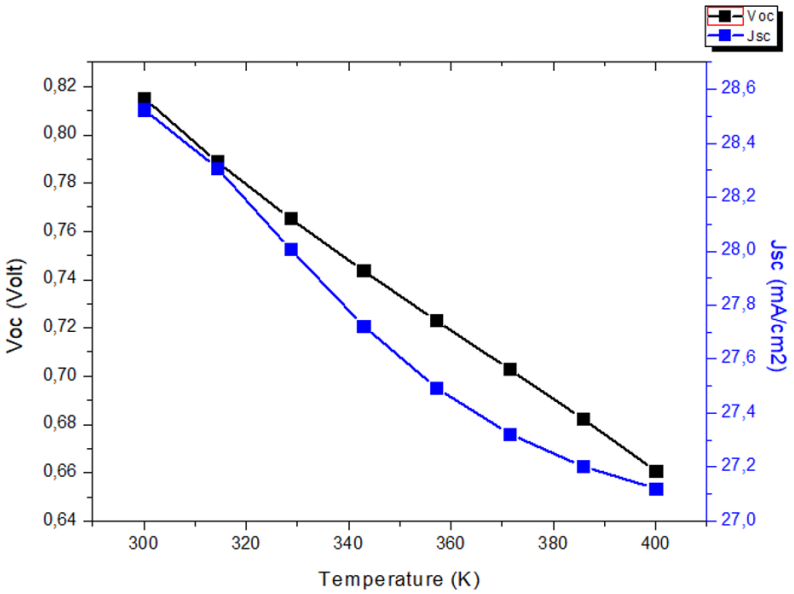

Figure 8. Variation of cell efficiency Voc and Jsc with temperature.

The combined effect of reduced Voc and Jsc with temperature culminates in a reduction of the overall efficiency (η) of the solar cell, as evidenced by the data presented. The efficiency declines from 16.7127% at 300 K to 13.906% at 400 K. This highlights the critical significance of thermal management in the design of solar cells, particularly those based on CZTS, to uphold performance

across varying environmental conditions. Furthermore, the balance between sustaining elevated Voc and Jsc whilst addressing temperature effects is essential for optimizing the design and material selection in these solar cells.

At lower temperatures (300 K to ~350 K), Figure 9 represents a progressive improvement of the fill factor (FF). This phenomenon can be ascribed to a diminution in the series resistance inherent in the solar cell as the temperature escalates. Series resistance, which originates from resistive losses along the current-conducting pathways, generally exhibits a decline with increasing temperature, facilitating augmented current flow and subsequently leading to an improvement in the FF.
As the temperature persists in rising beyond the optimal threshold, the FF commences a downward trajectory. This reduction is predominantly attributable to heightened recombination rates of charge carriers within the solar cell. At elevated temperatures, the increase in thermal energy culminates in an augmented rate of electron-hole recombination, especially within the depletion region and at defect sites. This phenomenon culminates in a reduction of the photocurrent available for energy conversion, thereby diminishing the FF.

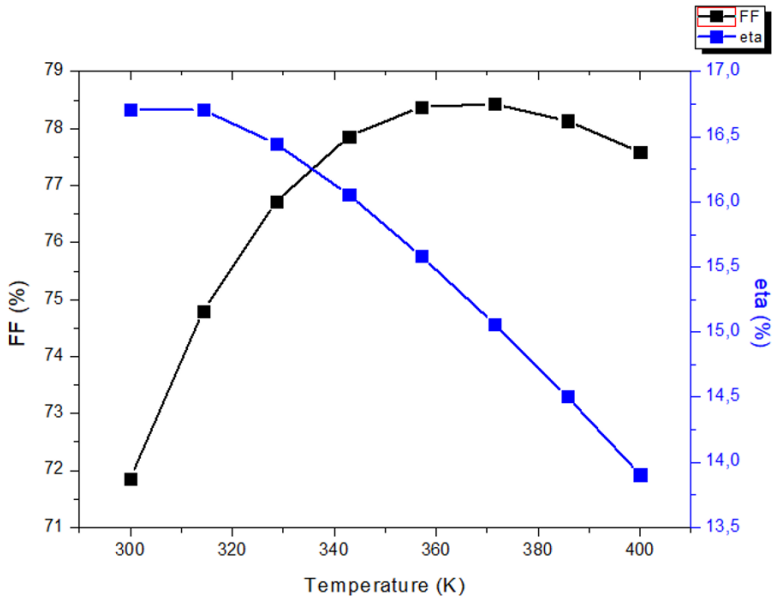

Figure 9. Variation of cell efficiency FF and eta with temperature.

The efficiency of the solar cell demonstrates a consistent attenuation concomitant with rising temperature. Efficiency is intricately linked to both the open-circuit voltage (Voc) and the FF. Nevertheless, temperature exerts a more pronounced influence on Voc, which experiences a substantial decline with increasing temperature. As the temperature elevates, the intrinsic carrier concentration of the semiconductor escalates, resulting in a shift of the Fermi level closer to the intrinsic level. This shift mitigates the disparity between the conduction band and the Fermi level, thereby leading to a reduction in Voc. Given that Voc possesses a logarithmic relationship with the ratio of light-generated current to dark saturation current, an increase in temperature induces an exponential rise in the dark saturation current, culminating in a reduced Voc and, as a result, diminished efficiency.
Considering that both FF and Voc are pivotal constituents of the efficiency, the convergence of declining FF and Voc engenders a substantial decrease in overall efficiency as temperature ascends. This effect is further exacerbated at elevated temperatures, wherein the decline in efficiency becomes markedly pronounced.
The discerned trends accentuate the criticality of thermal management within solar cell design.

To preserve high efficiency, it is imperative to mitigate temperature-induced losses. This objective can be accomplished through the utilization of materials with lower temperature coefficients for Voc or through structural optimizations aimed at reducing recombination losses under elevated temperature conditions. The selection of materials, particularly those employed in the active layer and contacts, is instrumental in determining the extent to which temperature influences the FF and efficiency. For example, materials characterized by higher bandgaps may provide increased Voc stability at elevated temperatures; however, such advantages may be accompanied by trade-offs in other parameters such as (Jsc). In conclusion, the diagram and data collectively elucidate that while the fill factor initially reaps benefits from moderate temperature elevations, both FF and efficiency are adversely affected at higher temperatures due to increased recombination and diminished Voc. These findings underscore the necessity for meticulous consideration of temperature effects in both the design and implementation of solar cells, particularly in contexts where they are subjected to elevated thermal loads [35].

4. CONCLUSION

In conclusion, the findings from the simulation emphasize the critical significance of optimizing layer thickness and regulating temperature to attain peak efficiency in solar cells. With regard to the CZTS layer, an ideal thickness promotes an increase in (Voc) by diminishing recombination and resistive losses, while concurrently sustaining elevated short-circuit current density (Jsc). An augmentation in thickness increases light absorption and Voc; however, it may concurrently lead to elevated recombination and resistive losses, thereby diminishing Jsc and overall efficiency. Likewise, for the MoS_2 layer, the optimal thickness increases both Voc and Jsc, although the increase in efficiency occurs at the cost of a diminished fill factor (FF) owing to heightened resistive losses. For the WSe_2 layer, an optimal thickness in the vicinity of 1 μm increases both FF and efficiency, yet further increases result in diminishing returns attributable to augmented recombination and resistive losses. Moreover, elevated temperatures exert a detrimental effect on Voc and Jsc, culminating in a reduction of efficiency. While FF initially benefits from rising temperatures due to a decrease in series resistance, it subsequently declines as a result of increased recombination. Consequently, effective thermal management and meticulous optimization of layer thickness are imperative for sustaining elevated performance and efficiency in solar cells across diverse conditions.

Authors contribution: The contributions of each author are as follows:
O.Belhaidouri:Conceptualization,methodology, writing - original draft and Data analysis.
R. Moultif: software, reviewing – editing and Supervision.
L. Mouakkir: Investigation and validation of results.
Ahmed. Hader: Supervision and project administration.
S. Rochd: Supervision and project administration.
Khadija.Mhada : validation of results , project administration
All authors read and approved the final manuscript.
Funding: The authors declare that this research received no external funding.
Data Availability Statement: Not applicable.
Conflicts of Interest: The authors declare that they have no competing interests related to this study. All authors have disclosed any potential conflicts of interest and have adhered to ethical standards in conducting the research.
Acknowledgements: The authors would like to thank Dr. M. Burgelman from University of Gent for using SCAPS-1D program in all simulations reported in this paper.

REFERENCES

[1] P. Tian, L. Tang, K. S. Teng, J. Xiang, and S. P. Lau, "Recent advances in graphene homogeneous p-n junction for optoelectronics," Adv. Mater. Technol., vol. 4, 2019, Art. no. 1900007, doi: https://doi.org/10.1002/admt.201900007.

[2] F. Encinas-Sanz and J. M. Guerra, "Laser-induced hot carrier photovoltaic effects in semiconductor junctions," Prog. Quant. Electron., vol. 27, pp. 267–294, 2003, doi: https://doi.org/10.1016/S0079-6727(03)00002-8.

[3] R. Frisenda, A. J. Molina-Mendoza, T. Mueller, A. Castellanos-Gomez, and H. S. J. van der Zant, "Atomically thin p-n junctions based on two-dimensional materials," Chem. Soc. Rev., vol. 47, pp. 3339–3358, 2018, doi: https://doi.org/10.1039/C7CS00880E.

[4] J. Ramanujam, D. M. Bishop, T. K. Todorov, O. Gunawan, J. Rath, R. Nekovei, E. Artegiani, and A. Romeo, "Flexible CIGS, CdTe and a-Si:H based thin film solar cells: A review," Prog. Mater Sci., vol. 110, 2020, Art. no. 100619, doi: https://doi.org/10.1016/j.pmatsci.2019.100619.

[5] T. D. Lee and A. U. Ebong, "A review of thin film solar cell technologies and challenges," Renew. Sustain. Energy Rev., vol. 70, pp. 1286–1297, 2017, doi: https://doi.org/10.1016/j.rser.2016.12.028.

[6] I. Massiot, A. Cattoni, and S. Collin, "Progress and prospects for ultrathin solar cells," Nat. Energy, vol. 5, pp. 959–972, 2020, doi: https://doi.org/10.1038/s41560-020-00714-4.

[7] Y. Lee, H. H. Tan, C. Jagadish, and S. K. Karuturi, "Controlled cracking for large-area thin film exfoliation: Working principles, status, and prospects," ACS Appl. Electron. Mater., vol. 3, pp. 145–162, 2021, doi: https://doi.org/10.1021/acsaelm.0c00892.

[8] M. Saifullah, S. Ahn, J. Gwak, S. Ahn, K. Kim, J. Cho, J. H. Park, Y. J. Eo, A. Cho, J. S. Yoo, and J. H. Yun, "Development of semitransparent CIGS thin-film solar cells modified with a sulfurized-AgGa layer for building applications," J. Mater. Chem. A, vol. 4, pp. 10542–10551, 2016, doi: https://doi.org/10.1039/C6TA01909A.

[9] J. Guo, W. H. Zhou, Y. L. Pei, Q. W. Tian, D. X. Kou, Z. J. Zhou, Y. N. Meng, and S. X. Wu, "High efficiency CZTSSe thin film solar cells from pure element solution: A study of additional Sn complement," Sol. Energy Mater. Sol. Cells, vol. 155, pp. 209–215, 2016, doi: https://doi.org/10.1016/j.solmat.2016.06.021.

[10] Y. Wei, K. Zhou, X. Meng, X. Sun, Z. Ma, Z. Li, and D. Zhuang, "Improving the performance of solution–based CZTSSe absorber by selenization annealing with selenium powder in argon," J. Alloy. Compd., vol. 976, 2024, Art. no. 173123, doi: https://doi.org/10.1016/j.jallcom.2023.173123.

[11] A. D. Saragih, W. Wubet, H. Abdullah, A. K. Abay, and D. H. Kuo, "Characterization of Ag-doped Cu2ZnSnSe4 bulk materials and their application as thin film semiconductor in solar cells," Mater. Sci. Eng. B, vol. 225, pp. 45–53, 2017, doi: https://doi.org/10.1016/j.mseb.2017.08.007.

[12] Y. Zhang, D. Jiang, Y. Sui, Y. Wu, Z. Wang, L. Yang, F. Wang, S. Lv, and B. Yao, "Synthesis and investigation of environmental protection and earth-abundant kesterite Cu2MgxZn1-xSn(S,Se)4 thin films for solar cells," Ceram. Int., 2018, doi: https://doi.org/10.1016/j.ceramint.2018.05.167.

[13] A. D. Saragih, W. Wubet, H. Abdullah, A. K. Abay, and D. H. Kuo, "Characterization of Ag-doped Cu2ZnSnSe4 bulk materials and their application as thin film semiconductor in solar cells," Mater. Sci. Eng. B, vol. 225, pp. 45–53, 2017, doi: https://doi.org/10.1016/j.mseb.2017.08.007.

[14] M. He, K. Sun, M. P. Suryawanshi, J. Li, and X. Hao, "Interface engineering of p-n heterojunction for kesterite photovoltaics: A progress review," J. Energy Chem., vol. 60, pp. 1–8, 2021, doi: https://doi.org/10.1016/j.jechem.2020.12.019.

[15] A. Ait Abdelkadir and M. Sahal, "Theoretical development of the CZTS thin-film solar cell by

SCAPS-1D software based on experimental work," Mater. Sci. Eng. B, vol. 296, 2023, Art. no. 116710, doi: https://doi.org/10.1016/j.mseb.2023.116710.

[16] Sadanand, D. K. Dwivedi, F. A. Alharthi, and A. El Marghany, "One-step hydrothermal synthesis of Cu2ZnSn(S,Se)4 nanoparticles: Structural and optical properties," Nanosci. Nanotechnol. Lett., vol. 12, pp. 338–344, 2020, doi: https://doi.org/10.1166/nnl.2020.3121.

[17] R. Kotipalli, O. Poncelet, G. Li, Y. Zeng, L. A. Francis, B. Vermang, and D. Flandre, "Addressing the impact of rear surface passivation mechanisms on ultra-thin Cu(In, Ga)Se2 solar cell performances using SCAPS 1-D model," Sol. Energy, vol. 157, pp. 603–613, 2017, doi: https://doi.org/10.1016/j.solener.2017.08.055.

[18] A. Kannaujiya, S. Kannaujiya, and R. K. Chauhan, "Effect of gate metal work function on leakage current in single pocket FDSOI 28 nm transistor," in 2021 Int. Conf. on Computational Science and Network Technology (CSNT), 2021, pp. 241–246, doi: https://doi.org/10.1109/csnt51715.2021.9509715.

[19] M. Burgelman, K. Decock, S. Khelifi, and A. Abass, "Advanced electrical simulation of thin film solar cells," Thin Solid Films, vol. 535, pp. 296–301, 2013, doi: https://doi.org/10.1016/j.tsf.2012.10.032.

[20] O. Belhaidouri, R. Moultif, L. Mouakkir, M. Karim, A. Hader, Y. Lachtioui, and O. Bajjou, "Optimizing CZTS solar cells efficiency using eco-friendly layers by SCAPS simulation," J. Adv. Res. Fluid Mech. Therm. Sci., vol. 119, no. 2, pp. 79–90, 2024, doi: https://doi.org/10.37934/arfmts.119.2.7990.

[21] J. B. You, X. W. Zhang, J. J. Dong, X. M. Song, Z. G. Yin, N. F. Chen, and H. Yan, "Localized-surface-plasmon enhanced the 357 nm forward emission from ZnMgO films capped by Pt nanoparticles," Nanoscale Res. Lett., vol. 4, pp. 1121–1125, 2009, doi: https://doi.org/10.1007/s11671-009-9366-y.

[22] Tripathi, Sadanand, and P. Lohia, "Contribution to sustainable and environmental friendly non-toxic CZTS solar cell with an innovative hybrid buffer layer," Sol. Energy, vol. 204, pp. 748–760, 2020, doi: https://doi.org/10.1016/j.solener.2020.05.033.

[23] A. Redinger and T. Unold, "High surface recombination velocity limits Quasi-Fermi level splitting in kesterite absorbers," Sci. Rep., vol. 8, Art. no. 19798, 2018, doi: https://doi.org/10.1038/s41598-018-19798-w.

[24] T. Ghorbani, M. Zahedifar, M. Moradi, and E. Ghanbari, "Influence of affinity, band gap and ambient temperature on the efficiency of CIGS solar cells," Optik, vol. 223, 2020, Art. no. 165541, doi: https://doi.org/10.1016/j.ijleo.2020.165541.

[25] D. K. Dwivedi and Sadanand, "Modeling of CZTSSe solar photovoltaic cell for window layer optimization," Optik, vol. 222, 2020, Art. no. 165407, doi: https://doi.org/10.1016/j.ijleo.2020.165407.

[26] V. Selamneni, S. K. Ganeshan, N. Nerurkar, T. Akshaya, and P. Sahatiya, "Facile fabrication of MoSe2 on paper as an electromechanical piezoresistive pressure-strain sensor," IEEE Trans. Instrum. Meas., vol. 70, 2021, doi: https://doi.org/10.1109/TIM.2020.3038003.

[27] H. B. Michaelson, "The work function of the elements and its periodicity," J. Appl. Phys., vol. 48, pp. 4729–4733, 1977, doi: https://doi.org/10.1063/1.323539.

[28] M. A. Green, "General temperature dependence of solar cell performance and implications for device modelling," Prog. Photovoltaics Res. Appl., vol. 11, pp. 333–340, 2003, doi: https://doi.org/10.1002/pip.496.

[29] K. Pandey, A. K. Patel, R. Mishra, "Numerical study on performance enhancement of CZTSSe solar cells with Cu_2O and $MoTe_2$ as hole transport layer," Journal of Computational Electronics, vol. 21, no. 4, pp. 895–904, 2022, doi: https://doi.org/10.1016/j.micrna.2022.207356.

[30] S. Mishra, K. Bhargava, D. Deb, "Numerical simulation of potential induced degradation (PID) in different thin-film solar cells using SCAPS-1D," Solar Energy, vol. 188, pp. 353–360, 2019, doi: https://doi.org/10.1016/J.SOLENER.2019.05.077.

[31] Z. Yan, G. Li, T. Li, S. Zhao, K. Yang, S. Zhang, M. Fan, L. Guo, B. Zhang, "Passively Q-switched Ho,Pr:LiLuF4 laser at 2.95 μm using MoSe2," IEEE Photonics Journal, vol. 9, 2017, doi: https://doi.org/10.1109/JPHOT.2017.2749328.

[32] H. B. Michaelson, "The work function of the elements and its periodicity," Journal of Applied Physics, vol. 48, pp. 4729–4733, 1977, doi: https://doi.org/10.1063/1.323539.

[33] V. Selamneni, S. K. Ganeshan, N. Nerurkar, T. Akshaya, P. Sahatiya, "Facile fabrication of $MoSe_2$ on paper as an electromechanical piezoresistive pressure-strain sensor," IEEE Transactions on Instrumentation and Measurement, vol. 70, 2021, doi: https://doi.org/10.1109/TIM.2020.3038003.

[34] J. Zhang, L. Shao, "Cu_2ZnSnS_4 thin films prepared by sulfurizing different multilayer metal precursors," Science in China Series E: Technological Sciences, vol. 52, pp. 269–272, 2009, doi: https://doi.org/10.1007/s11431-009-0013-8.

[35] A. Kumar, A. D. Thakur, "Improvement of efficiency in CZTSSe solar cell by using back surface field," in IOP Conference Series: Materials Science and Engineering, vol. 360, p. 012027, IOP Publishing, 2018, doi: https://doi.org/10.1088/1757-899X/360/1/012027.